Influence of Porosity on Flame Speed in Gasless Bimetallic Reactive Systems

Hesam Akbarnejad[a], Antoine Bacciochini[a], Julian Lee[b], and Matei I.Radulescu[a]

[a]Department of Mechanical Engineering, University of Ottawa, Ottawa, Canada

[b] Defence Research and Development Canada, Suffield, Canada

1 Introduction

Gasless reactive materials are often composed of intermetallic mixtures. These materials have energy densities comparable or higher than conventional energetic materials [1]. Reaction wave propagation in gasless reactive materials are believed to rely mainly on the heat transport by thermal conduction [2], yielding speeds on the order of 10^{-2} m/s, and rarely exceeding 1 m/s in certain mixtures [3]. Gasless detonations have been theorized by Bennett & Horie [4], but require materials with vanishing porosity. The modest product expansion of gasless products needs to overcome the porosity to drive the shock in a detonation wave.

Conventional intermetallic reactive materials are prepared in powder form. Powder compacts have characteristic densities ranging from approximately 30% to 75% of the theoretical maximal density. These mixtures have now been well characterized. Very recently, Bacciochini et al. have developed a technique to prepare materials with vanishing porosity [5]. They used the "Cold Gas Dynamic Spray Process" process. In cold spraying technique, particles are accelerated to high speeds with a relatively low temperature. The powders are merged together via plastic deformation upon impact resulting mixtures with porosity levels close to zero. Bacciochini et al. measured flame speeds in their compacts higher by more than an order of magnitude as compared with the high porosity powder compacts. The reason for this very large difference was not reported. The present study addresses the influence of density of the compacts on the reaction wave propagation speed.

The compaction of the material may have different physical influences on the reaction wave and its structure. For example, the closer contact between the constituents may provide more efficient mass transfer. Likewise, the heat transfer by conduction may also be improved. The spray consolidation further deforms the powder, potentially providing further mechanical activation. The present study thus attempts to isolate the main mechanism controlling the reaction wave enhancement with density increase. Experiments are performed in aluminum nickel mixtures (Al-Ni). The reactions between aluminum and nickel powders are reported to be gasless [2] and therefore, the effect of heat convection is negligible. Milled powders are also considered in order to compare with the results obtained by Bacchiochini et al. at nearly 100% TMD. The investigation rests on the analytical model formulated by

Correspondence to: hakba024@uottawa.ca

Makino [2]. Makino's model takes into account the role of mass diffusion at the boundaries of the two non-premixed metallic components and the regression rate of the metal with the highest melting point. As it treats this process separately from the heat diffusion process, one can test the modifications in heat transfer mode and reaction kinetics separately and isolate the main mechanism at play in densified inter-metallic energetic materials.

2 Experimental Details

The experiments focused on the equimolar mixture of aluminum and nickel. Fig. 1 shows a photograph of the raw powders used, with a dimension on the order of a few microns.

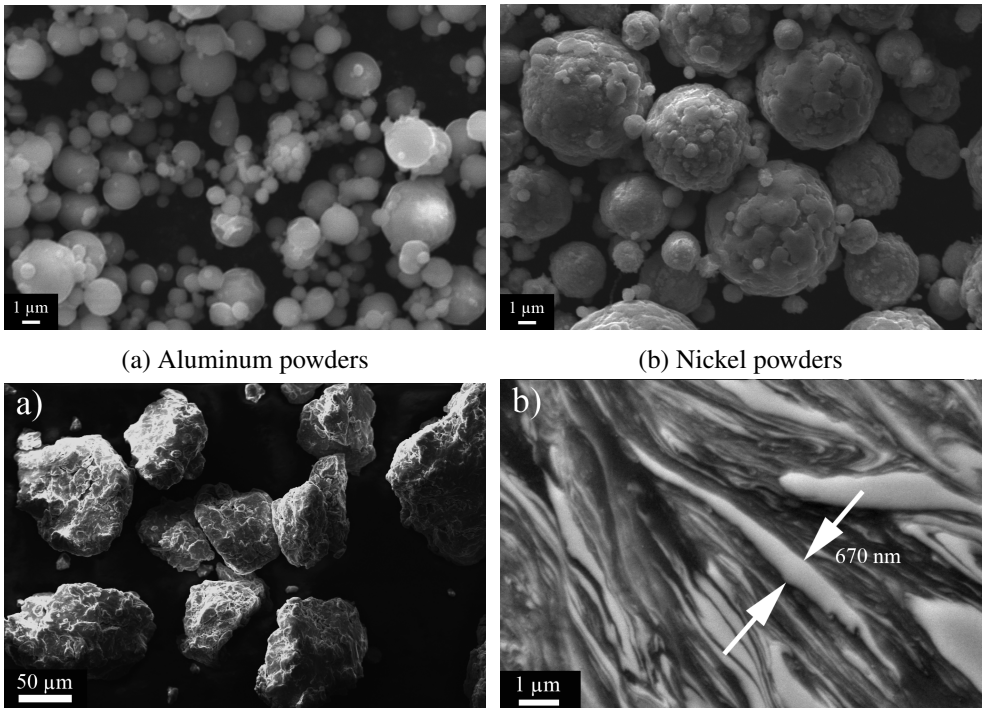

(a) Aluminum powders (b) Nickel powders

(c) Milled Al-Ni (d) Zoom in view of milled Al-Ni

Figure 1: Scanning electron micrograph of the structure of the Al-Ni [5]

Experiments were also performed in milled mixtures, following the same process presented by Bacciochini et al. [5]. Ball milling permitted to refine the structure of the intermetallic mixture and control its reactivity. Dry planetary milling was used to refine the structure of intermetallic mixtures of Al-Ni in an inert argon atmosphere. The milling process permitted us to refine the structure of the materials. Figs. 1c and 1d show scanning electron microscope (SEM) records of the Al-Ni after milling. The milled powders consist of dense irregular shaped grains (Fig. 1c) with a lamellar inner structure (Fig. 1d). The lamellar structure of elongated layers of nickel of less than 500 nm can be found in the aluminum matrix.

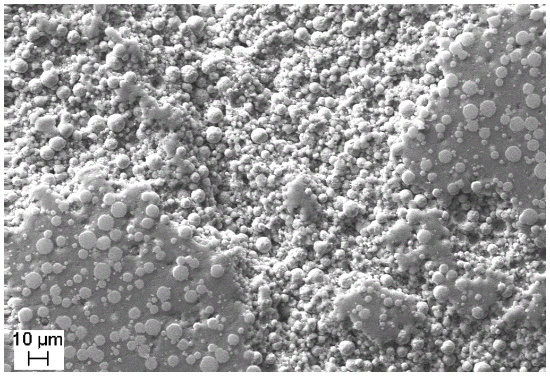

(a) Non-milled Al-Ni $\rho_{rel} = \%78$

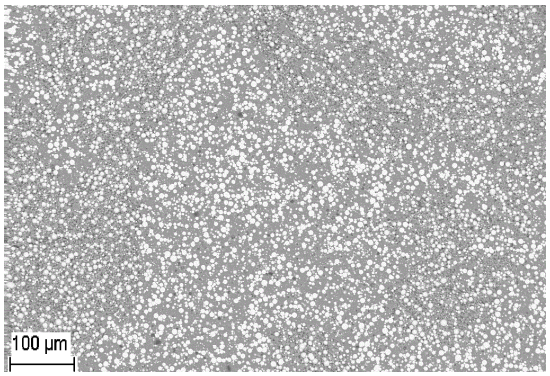

(b) Non-milled Al-Ni $\rho_{rel} = \%78$

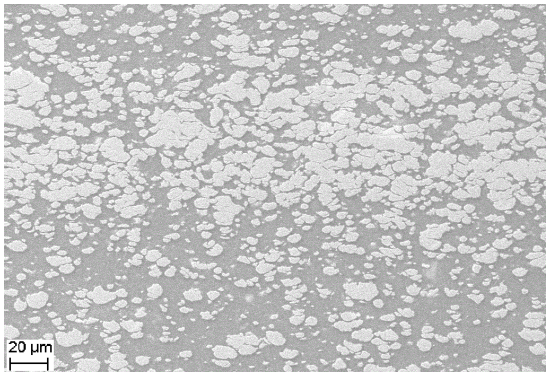

(c) Non-milled Al-Ni $\rho_{rel} \approx \%100$

Figure 2: Scanning electron micrograph of the structure of the Al-Ni at different density ratios

The flame speed measurements were performed in metallic channels of square cross-section containing male and female sides. Powders were placed in the female part and compacted using the male part. Different compaction forces were used. These were achieved with different equipment, such as a hammer, hand press, and a hydraulic press. The force required to compact the powders below %60 TMD was in the range of 0N to 1KN. Above approximately %60 TMD, a much larger compaction was required, generally in excess of 20KN. The density of %60 TMD thus corresponds to the critical density above which severe plastic deformation is required to further compact the powders. The scanning electron microscopy of the powders after plastic deformation and close to the theoretical maximum density are shown in Fig. 2. Comparing the structure of undeformed non-milled powders (Figs. 1a and 1b) and deformed non-milled powders at %78 TMD (Figs. 2a and 2b), we can observe that original spherical shapes of the nickel powders are remained while the aluminum powders at %78 TMD are deformed. As a result, after deformation of the particles, a higher contact surface between the powders has been formed. Near 100% TMD, both aluminum and nickel powders are deformed and therefore, the contact surface is much larger at 100% TMD (Fig. 2c) as compared to higher porosity mixtures.

Experiments were performed in different channel sizes in order to determine the influence of losses on the burning speed. Steel channels with 0.1cm, 0.25 cm, 0.5 cm and 1 cm cross-section grooves were used. A high speed camera captured the flame propagation along the length of the channel. Analysis of the sequential frames permitted us to obtain the flame speed.

In order to determine the thermal conductivity dependence on the density, the thermal conductivity of Al-Ni powders was experimentally measured using the steady state divided bar technique. A sketch of the set-up is shown in Fig. 3. A 25 mm-thick layer of powders was contained in a thin-walled steel capsule between two control cylindrical blocks of 25 mm in diameter. In order to ensure an approximately

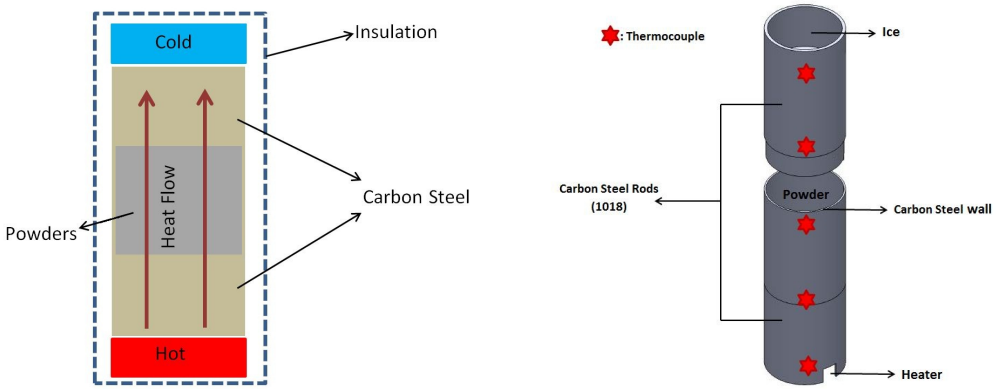

Figure 3: Experimental set-up used to measure the thermal conductivity

axial heat flux, the assembly was insulated radially. Electrical heaters were imposed at one extremity, while the opposing surface was kept at constant temperature by continuous addition of melting ice. Thermocouples placed along the assembly permitted us to measure the axial heat flux in the control layers, and deduce the conductivity in the powder layer.

3 Results

Fig. 4 shows examples of the type of flame propagation observed in gasless systems where the flame is initiated from the left and travels to the right. While the flame propagation shown in Fig. 4a shows a stable propagation for the non-milled Al-Ni system, the ball-milled system shown in Fig. 4a exhibits localized bursts of the powders, partially ejecting them out of the channel. Although, the exact reason behind this behavior is not clear, gases trapped in the milled mixtures can be responsible for this material ejection.

The experimental flame speeds calculated from the recordings of the flame are presented in Fig. 5 for different channel sizes. We have found a very weak dependence of the flame speed on the channel size, typically smaller than the scatter in the measurements themselves. Losses to the walls can thus be neglected. Inspection of Fig. 5 also shows the influence of ball milling on the reaction wave characteristics. The flame speed increases by approximately a factor of 4. Also the dependency of the flame speed to the porosity of the mixture can be seen in this graph. Flame speed seems to gradually increase by increasing the density for low density mixtures. However, a sudden change of flame speed is observed at approximately $\rho_{rel} = 0.6$.

We attempted to determine whether the observed trends were due to the mass diffusion enhancement, or to the heat diffusion enhancement by comparing the results with the quantitative model of Makino. The input parameters required are the mixture density, conductivity and characteristic powder dimension. While the density and powder dimension are readily available for the tests performed, the conductivity is not. It is well known that conductivity of compacted powders is dependent of the type and morphology of powders used.

The conductivity of densified powders approaching TMD can be accurately predicted by available models. Fig. 6 shows the comparison between the Effective Medium Theory (EMT) [6], the well known Maxwell model of swiss-cheese like porous materials, and the conductivity of parallel layered structures, where the lower conductivity comes from a lower equivalent cross-sectional area of the material. Above approximately 60% TMD, these models predict very similar conductivities.

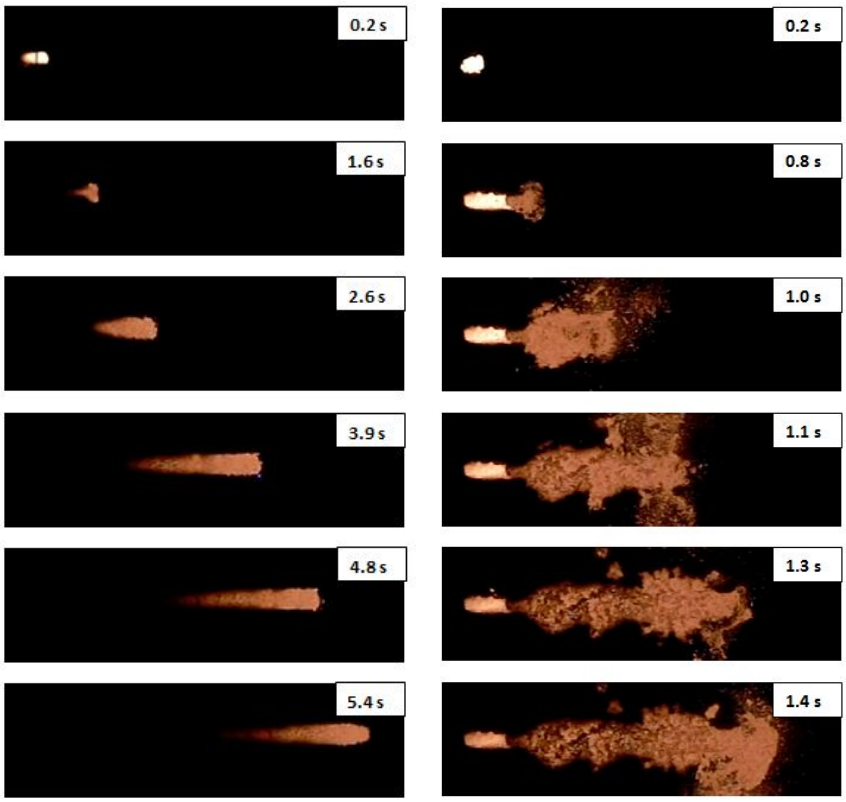

(a) Non-milled powders (b) Ball milled powders

Figure 4: Sequential flames illustrating the flame propagation in Al-Ni system in the 0.75 cm channel width

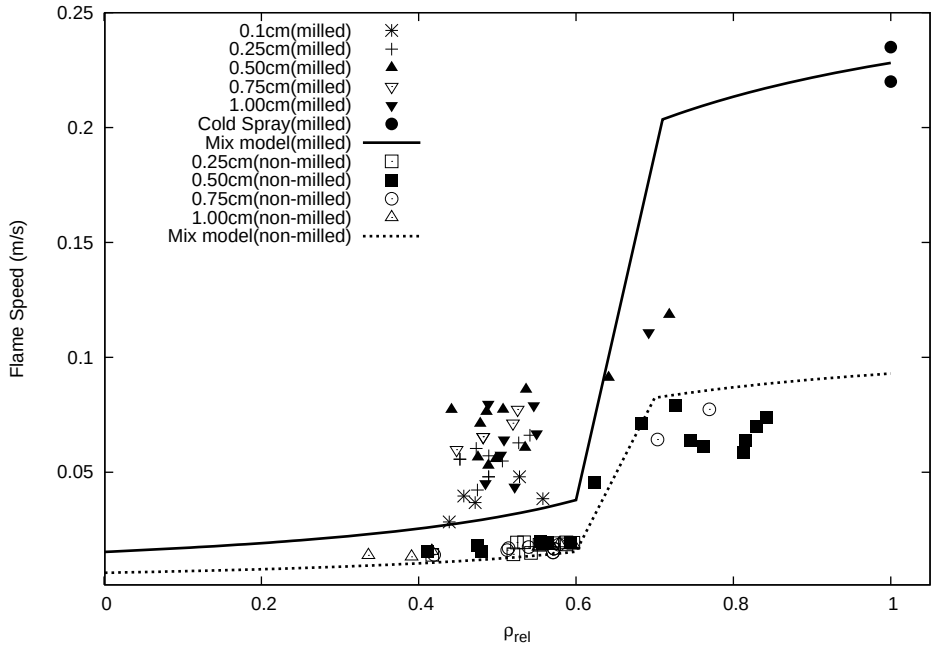

Figure 5: Measured flame speeds in milled and non-milled Al-Ni as function of relative density and comparison with improved Makino's model

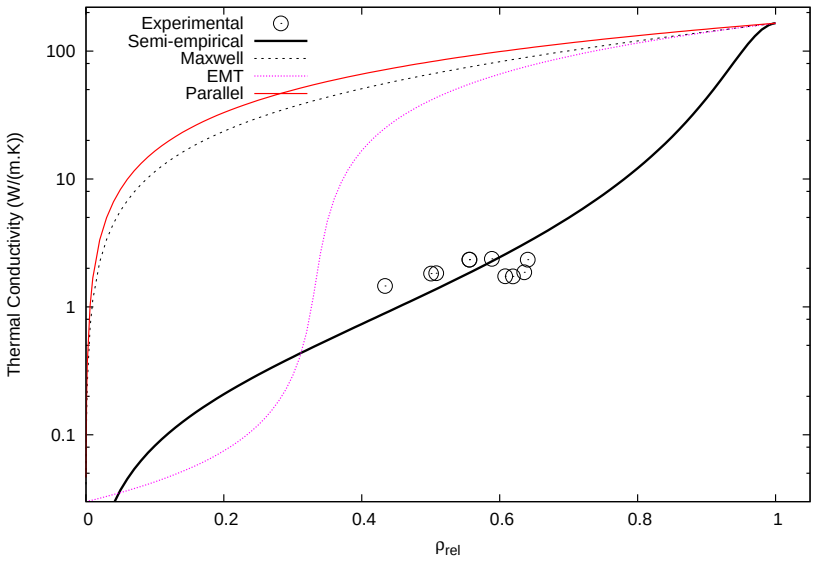

Figure 6: Measured thermal conductivity of Al-Ni powders and comparison with different theoretical models

For low %TMD (high porosity), however, the models diverge. This reflects the importance of the powder morphology in the heat conduction mechanism. Our experiments of heat conductivity are also shown in the Fig. 6. While they do not agree with any of the models considered, they show that the heat conductivity is lower than in materials with interior porosity, such as those modeled by the Maxwell model, by more than an order of magnitude.

For the comparison of flame speed data with Makino's model, we thus use different conductivity for the high and low density powders, respectively. For the low density powders, we fit the semi-empirical model suggested by Aivazov and Domashnev [7] to our experimental data. At higher densities, where most models agree, we use the analytical expression provided by the Effective Medium Theory (EMT) [6].

Using Makino's model, the flame speed can then be related to the density of the mixture via the dependence of thermal conductivity on density:

$$S_u \propto \sqrt{\frac{K(\rho_{rel})}{\rho_{rel}}} \tag{1}$$

where the thermal conductivity $K(\rho_{rel})$ is estimated separately for low and high densities using the semi-empirical and the EMT models respectively. The thermo-chemical parameters we use are those proposed by Makino. From Makino's model, the flame speed is inversely proportional to the particle sizes represented by an average radius R. For the non-milled powders, we took a particle size of $R = 2\mu m$, consistent with the characteristic size of the powders observed from the scanning electron micrographs. For the milled powders, the particle sizes cannot easily be estimated from the scanning electron micrograph. For comparison purposes, taking an average particle size of $R = 0.8\mu m$ provides an excellent agreement with the measured flame speeds.

Predictions made with Makino's model for the flame speeds in the Al-Ni system are shown in Fig. 5. In both the non-milled and milled Al-Ni samples, the effect of density is well reproduced by the model.

We can thus conclude that the density effect observed previously by Bacciochini et al. is mainly due to an enhancement of the heat conductivity in densified powder compacts.

References

[1] S. Fischer and M. Grubelich, "Theoretical energy release of thermites, intermetallics and combustible metals," in *24th International Pyrotechnics Seminar, Monterey California*, 27-31 July 1998, pp. 231–286.

[2] A. Makino, "Fundamental aspects of the heterogeneous flame in the self-propagating high-temperature synthesis (shs) process," *Progress in Energy and Combustion Science*, vol. 27, no. 1, pp. 1–74, 2001.

[3] A. S. Rogachev, "Exothermic reaction waves in multilayer nanofilms," *Uspekhi Khimii*, vol. 77, no. 1, pp. 22–38, 2008.

[4] L. S. Bennett and Y. Horie, "Shock induced inorganic reactions and condensed phase detonations," *Shock Waves*, vol. 4, pp. 127–136, 1994.

[5] A. Bacciochini, M. Radulescu, Y. Charron-Tousignant, J. Van Dyke, M. Nganbe, M. Yandouzi, J. J. Lee, and B. Jodoin, "Enhanced reactivity of mechanically-activated nano-scale gasless reactive materials consolidated by coldspray," *Surface and Coatings Technology*, vol. 206, pp. 4343–4348, 2012.

[6] J. Carson, S. J. Lovatt, D. J. Tanner, and A. C. Cleland, "Thermal conductivity bounds for isotropic, porous materials," *International Journal of Heat and Mass Transfer*, vol. 48, no. 11, pp. 2150 – 2158, 2005.

[7] M. I. Aivazov and I. A. Domashnev, "Influence of porosity on the conductivity of hot-pressed titanium-nitride specimens," *Powder Metallurgy and Metal Ceramics*, vol. 7, pp. 708–710, 1968.